J Neurophysiol 100: 1087–1097, 2008.
First published June 25, 2008; doi:10.1152/jn.90527.2008.

Complex Temporal Response Patterns With a Simple Retinal Circuit

Birgit Werner,[1] Paul B. Cook,[1,2] and Christopher L. Passaglia[1,3]
[1]*Program in Neuroscience,* [2]*Department of Biology, and* [3]*Department of Biomedical Engineering, Boston University, Boston, Massachusetts*

Submitted 3 May 2008; accepted in final form 21 June 2008

Werner B, Cook PB, Passaglia CL. Complex temporal response patterns with a simple retinal circuit. *J Neurophysiol* 100: 1087–1097, 2008. First published June 25, 2008; doi:10.1152/jn.90527.2008. The retina can respond to a wide array of features in the visual input. It was recently reported that the retina can even recognize complicated temporal input patterns and signal violations in the patterns. When a sequence of flashes was presented, ganglion cells exhibited a variety of firing profiles and many cells showed an "omitted stimulus response" (OSR), in which they fired strongly if a flash in the sequence was omitted. We examined the synaptic origins of the OSR by recording excitatory synaptic currents from ganglion cells in the salamander retina in response to periodic flash sequences. Consistent with previous spike recordings, ganglion cells exhibited an OSR in their current response and the OSR shifted in time with a change in flash frequency such that it could predict when the next flash should have occurred. Although the behavior may seem sophisticated, we show that a simple linear–nonlinear model with a spike threshold can account for the OSR in ON ganglion cells and that the variety of complex firing profiles seen in other ganglion cells can be explained by adding contributions from the OFF pathway. We discuss the physiological and simulation results and their implications for understanding retinal mechanisms of visual information processing.

INTRODUCTION

Many studies have emphasized the diversity of response patterns among ganglion cells in the retina (Carcieri et al. 2003; Fairhall et al. 2006; Greschner et al. 2006; Rockhill et al. 2002; Segev et al. 2006). For some ganglion cell types the response patterns can be well characterized using linear methods. Other cell types produce more complicated response patterns. For example, in the mammalian retina, certain subpopulations of W-type cells respond both to the onset and offset of light (Cleland and Levick 1974; Stone and Fukuda 1974), whereas Y-type cells and other W-type cells exhibit both linear and nonlinear response properties (Enroth-Cugell and Robson 1966; Troy et al. 1995). In the salamander retina ON–OFF cells constitute the vast majority of ganglion cells (Burkhardt et al. 1998; Mittman et al. 1990) and pharmacological dissection of its retinal circuitry has shown that the ON–OFF behavior results from asynchronous and possibly rectified excitatory synaptic inputs from the ON and OFF pathways (Belgum et al. 1983; Pang et al. 2002; Wunk and Werblin 1979). Nonlinear circuit elements present a challenge for classifying neurons and gaining insight into network operation because they obscure the relationship between stimulus and spike response (Abbott and Chance 2002; Mechler and Ringach 2002).

Recently, it was reported that ganglion cells in the salamander retina can detect and predict periodic temporal patterns (Schwartz and Berry 2008; Schwartz et al. 2007). After a sequence of flashes many ganglion cells showed a strong spiking response more than one stimulus period after the last flash, as if the cell was anticipating the next flash and signaling its absence. The response was called an "omitted stimulus response" (OSR) and was reported to shift in time in accordance with the flash rate. The mechanism of OSR generation did not involve inhibition from amacrine cells, although ON bipolar cells were required. These results are surprising because temporal pattern recognition is regarded as a high-level computation that presumably takes place within the visual cortex and not at the earliest stage of vision and because the underlying computational elements within the retina are not amacrine cells, the most diverse cell class about which the least is known.

In this study we demonstrate how a simple, although nonlinear, retinal circuit can explain the OSR and other complex-looking response patterns to a flash sequence. We start by presenting recordings of the excitatory synaptic currents in salamander retinal ganglion cells and show that most cells receive inputs from both the ON and the OFF pathways, with the ON and the OFF contributions varying from cell to cell. We find that ganglion cells having a strong ON component in their current response always exhibit an OSR and that pharmacologically blocking the ON pathway abolishes the OSR, whereas the OSR remains after blocking inhibition from amacrine cells. We then simulate the response pattern of ON ganglion cells to a flash sequence using a linear–nonlinear (LN) model and show that the model predicts an OSR in every case. We also simulate ON–OFF cell behavior by including a second LN model for the OFF pathway and show the two-pathway model can produce not only an OSR but many of the complex response patterns that have been described for retinal ganglion cells to a temporal stimulus sequence (Schwartz and Berry 2008; Schwartz et al. 2007). According to our model, the OSR is not a response to an omitted flash but a byproduct of temporal integration across several flashes.

METHODS

Preparation

Larval tiger salamanders were purchased from Charles Sullivan (Nashville, TN) and were kept at 4°C on a 12-h light–dark cycle. Care and euthanization of the animals were carried out in accordance with procedures approved by Boston University Animal Care and Use

Address for reprint requests and other correspondence: B. Werner, Program in Neuroscience, 24 Cummington St., Boston, MA 02215 (E-mail: birgit.werner@gmail.com).

The costs of publication of this article were defrayed in part by the payment of page charges. The article must therefore be hereby marked "*advertisement*" in accordance with 18 U.S.C. Section 1734 solely to indicate this fact.

Committee. Retinal slices were prepared under infrared illumination. After removal of the cornea, iris, lens, and vitreous, the eye cup was cut into two rectangular pieces and placed ganglion cells down on two pieces of filter paper. The sclera together with the pigment epithelium was carefully lifted, so that only the retina stayed attached to the filter paper. The preparation was then cut into 300-μm-thick slices.

Electrophysiology

Light-evoked currents were recorded from cells in the ganglion cell layer (Werner et al. 2008). The preparation was continuously perfused with Ringer solution containing (in mM): 112 NaCl, 2 KCl, 2 $CaCl_2$, 1 $MgCl_2$, 5 glucose, and 5 HEPES, adjusted to pH 7.75 with NaOH. Drugs were added using an eight-channel microperfusion system. Strychnine (STR), picrotoxin (PTX), and imidazole-4-acetic acid (I4AA) were purchased from Sigma (St. Louis, MO). L-2-Amino-4-phosphonobutyrate (L-AP4) was purchased from Tocris (Ellisville, MO). Recordings were performed with a Multiclamp 700A patch-clamp amplifier (Axon Instruments, Foster City, CA). Data were filtered at 400 Hz and sampled at 1 kHz. Whole cell recordings were performed with electrodes pulled from borosilicate glass (World Precision Instruments, 1B150-4) with a P-97 Flaming/Brown micropipette puller. The solution inside the electrode contained (in mM): 100 K-gluconate, 1 $MgCl_2$, 1 EGTA, 10 HEPES, 4 ATP-K_2, 0.5 GTP-Na_3, and 8 KCl. For some cells perforated-patch recordings were performed. For these cells the intracellular solution contained K-aspartate instead of K-gluconate and ATP and GTP were left out. Furthermore, amphotericin-B was added to the electrode just before use. No differences in results were observed so the data were combined.

Light stimulation

Visual stimuli were programmed in Matlab (The MathWorks, Natick, MA) using the Psychophysics Toolbox (Brainard 1997) and projected onto the retina using a Lucivid image injector (MBF Bioscience). A Bits++ Digital Video Processor (Cambridge Research Systems) was used to obtain a 14-bit luminance range and to synchronize stimulus presentation with data collection. For step responses, a bright or dark bar (width 115–460 μm) of 100% contrast was presented on a steady uniform background (luminance = 8×10^4 photons$\cdot\mu m^{-1}\cdot s^{-1}$; size: 1.84 $\times$ 1.38 mm). Random binary noise sequences of 80% contrast were presented at 30 Hz. Flash sequences consisted of 16 flashes of 50-ms duration presented at frequencies ranging from 6 to 15 Hz.

Analysis

Data analysis was performed using Matlab. For every cell an ON–OFF index was determined from the step response according to the following formula

$$\text{ON–OFF} = (R_{ON} - R_{OFF})/(|R_{ON}| + |R_{OFF}|)$$

R_{ON} and R_{OFF} are the integrals of the current responses during the first 500 ms after the onset of a bright or dark flash, respectively, subtracted by the integrals of the response 500 ms before the beginning of the flash. The OSR to a sequence of flashes was defined as an excitatory current response that occurred later than one period after the last flash. The amplitude of the OSR was specified by the peak current after low-pass filtering the response at 30 Hz. The response of ON cells to white noise stimulation was analyzed with a standard LN model consisting of a linear filter followed by a static nonlinearity. The linear filter was calculated by cross-correlating the response of a cell to several minutes of stimulation with a binary noise luminance sequence. After calculating the linear filter, the static nonlinearity was formulated by plotting the current response of the cell at each point in time against the predicted response, which was determined by convolving the stimulus with the linear filter.

ON–OFF model

In our ON–OFF model, each pathway is described by an LN model consisting of a linear filter followed by a static nonlinearity and the summed signal is passed through a spike threshold (Fig. 7*A*). The model is described by *Eqs. 1–5*. The current response in the ON and the OFF pathways is computed by convolving the linear filter f(t) with the stimulus s(t) as given by *Eqs. 1* and *2*. The static nonlinearity in each pathway is described by two linear functions, the slopes of which (α, β) are the gain of the current response above and below zero (see *Eq. 3*). The outputs of the two linear–nonlinear pathways are summed to obtain the overall current response of the cell (*Eq. 4*). A spike threshold is then applied to model the spiking response of the cell (*Eq. 5*)

$$c_{ON}(t) = N_{ON}[s(t) * f_{ON}(t)] \quad (1)$$

$$c_{OFF}(t) = N_{OFF}[s(t) * f_{OFF}(t)] \quad (2)$$

$$\text{If } x < 0: \quad N(x) = \alpha_{ON} x$$

$$\text{If } x \geq 0: \quad N(x) = \beta_{ON} x \quad (3)$$

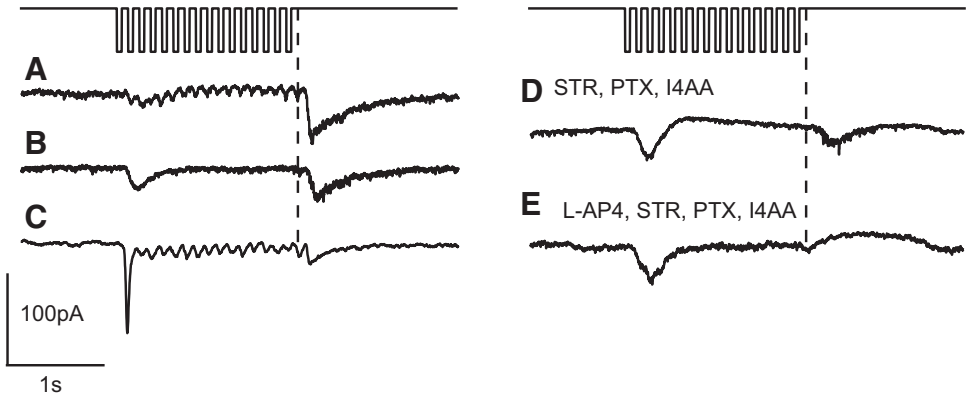

FIG. 1. The excitatory current responses of ganglion cells to a sequence of dark flashes (presented at 8.6 Hz) show an omitted stimulus response (OSR) after the offset of the sequence (*A*, *B*, *C*). Flashes are shown on the *top* and the time when the next flash would have occurred is indicated by a dashed line. Different cells vary in their response characteristics: *A*: responses throughout the sequence without strong onset response. *B*: responses occur only at the beginning and the end of the sequence. *C*: strong response at the beginning, responsive in the middle, weak OSR. *D*: OSR persists after blocking amacrine cell inhibition. *E*: L-2-amino-4-phosphonobutyrate (L-AP4) removes the OSR. Current traces show the average of 3–6 trials.

$$c(t) = c_{ON}(t) + c_{OFF}(t) \quad (4)$$

$$\text{If } c(t) \geq \gamma: \quad r(t) = 0$$

$$\text{If } c(t) < \gamma: \quad r(t) = c(t) - \gamma \quad (5)$$

The shape of the linear filters was based on measured current responses of ON and OFF ganglion cells to white noise stimulation. To compare simulations with Schwartz and Berry 2nd (2008), the width of the filters was scaled to better match the response speed under the conditions of their experiments.

RESULTS

Excitatory postsynaptic currents of many salamander ganglion cells exhibit an omitted stimulus response

We recorded the excitatory postsynaptic currents (EPSCs) of 36 cells in the ganglion cell layer in the retinal slice preparation in response to a sequence of 16 dark flashes presented at different frequencies. To isolate the EPSCs we held the voltage near the chloride reversal potential (−60 mV). At a flash frequency of 8.6 Hz, 92% of cells responded with an EPSC after the offset of the flash sequence. In all, 81% responded at the beginning of the sequence and 33% were responsive in the middle, whereas the others responded only at the beginning or the end of the flash sequence at this frequency (Fig. 1, *A–C*). In reference to earlier studies (Schwartz and Berry 2008; Schwartz et al. 2007), we call a current response that occurred later than one period after the last flash of the sequence an OSR. Of the 33 responses after the offset of the flash sequence, all were classified as an OSR. Some cells, however, also showed an additional response after the stimulus offset that would not classify as an OSR (Fig. 1, *A* and *C*).

We applied strychnine (2 μM), picrotoxin (100 μM), and imidazole-4-acetic acid (10 μM) to block GABAergic and glycinergic inhibition. Consistent with results from extracellular recordings (Schwartz and Berry 2nd 2008), the OSR remained after blocking amacrine cell inhibition (Fig. 1*D*).

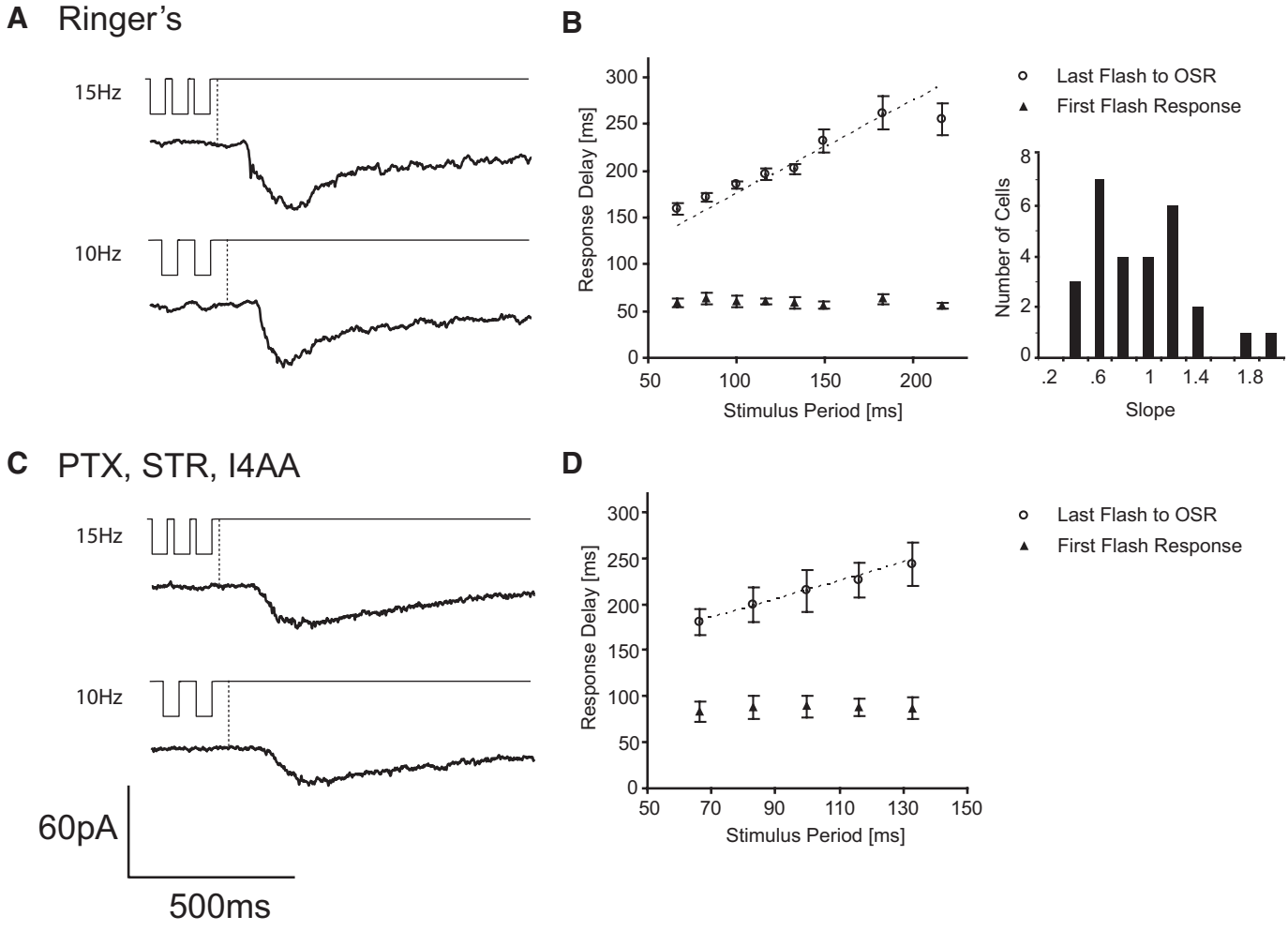

FIG. 2. The OSR shifts linearly with the flash period. *A*: excitatory postsynaptic current (EPSC) of a ganglion cell following a 15-Hz (*top*) and a 10-Hz (*bottom*) sequence of 16 dark flashes. The dotted line indicates the onset time of the missing flash. *B*: response delay plotted against the stimulus period (n = 28; not every cell was tested at all stimulus periods, but each was tested at ≥3 different periods). Error bars indicate SEs. The delay of the response after the last flash increases linearly with stimulus period (circles). The response delay after the first flash remains constant (triangles). The dotted line has a slope of one. The bar diagram on the *right* gives the distribution of measured slopes in individual cells binned into intervals of width 0.2. *C*: EPSCs of a ganglion cell to a 15- and 10-Hz flash train after application of picrotoxin (PTX), strychnine (STR), and imidazole-4-acetic acid (I4AA). *D*: same as in *B*, but after application of PTX, STR, and I4AA (n = 4). Different cells were used for the experiments in *B* and *D*. The effectiveness of the antagonists was confirmed with flash responses recorded before and after drug application.

However, adding L-2-amino-4-phosphonobutyrate (5 μM), which is known to block the synapse between photoreceptors and ON bipolar cells, eliminated the OSR (Fig. 1*E*).

Onset of the omitted stimulus response shifts with flash frequency

We measured the time from the onset of the last flash to the onset of the OSR for different flash frequencies. The OSR latency increased with the stimulus period with an average slope of 0.85 (SD = 0.40, n = 28) (Fig. 2, *A* and *B*), which is somewhat less than the slope of one reported for spike recordings (Schwartz et al. 2007). The distribution of slopes ranged widely across cells from 0.21 to 1.87 (Fig. 2*B*, bars). The latency of the response to the first flash was, by comparison, relatively independent of stimulus period (Fig. 2*B*, triangles). Blocking amacrine cell inhibition did not affect the temporal shift of the OSR with flash frequency (mean slope = 0.91, SD = 0.24, n = 4) (Fig. 2, *C* and *D*).

Offset response to a long flash is similar to the omitted stimulus response to a sequence of short flashes

To test whether the OSR uses the same mechanisms as the offset response to a luminance step we recorded the EPSCs in response to a 2-s-long dark flash. Figure 3, *A–D* shows examples of the current responses of four different cells to a flash sequence at 8.6 Hz (*top row*) and to a 2-s-long flash (*bottom row*). The cell in Fig. 3*A* is an OFF cell and therefore responds only with an excitatory current at the onset of the dark flash. Figure 3, *B* and *C* shows ON–OFF cells, with cell B being more OFF-dominated than cell C. Figure 3*D* shows an ON cell, which responds only to the offset of a dark flash. It may be seen from comparing the *top* and *bottom traces* that the responses to a single flash and a flash sequence clearly resemble each other in their overall shape. In Fig. 3*E* the peak amplitude of the OSR is plotted against the peak amplitude of the offset response of 37 cells. We found that the OSR amplitude is positively correlated (r = 0.6) with that of the offset response to a dark flash. This indicates that the OSR might not be the response to a missing flash, but the offset response to a dimming stimulus. At high flash frequencies the temporal integration window of the cell spans several flashes, which causes the response to a flash sequence to increasingly resemble that to a single long flash.

A linear–nonlinear model predicts the omitted stimulus response in ON ganglion cells

Responses of ON ganglion cells are often described by an LN model (Chichilnisky 2001; Kim and Rieke 2001). If the OSR is effectively the offset response to a dark flash, does this model then produce an OSR? We determined the LN model for four ON cells by recording their current responses to white noise stimulation. In every case the model predicted an OSR in response to a sequence of dark flashes. Figure 4 shows the linear filter and static nonlinearity measured for two ON ganglion cells and the LN model's prediction for a dark flash as well as a flash sequence. Although the model tends to underestimate the response amplitude, it captures the overall features of both waveforms. We next examined whether the model would also predict a temporal shift of the OSR with a change in flash frequency.

Figure 5*A* shows the OSR obtained through convolving various flash sequences with the linear filter and applying the static nonlinearity. The model predicts a delay in the onset of the response with an increase of the flash period (Fig. 5, *A* and *B*, diamonds). If a spike threshold is now applied to the current waveform (Fig. 5, *A* and *B*, filled symbols), the model shows that the higher the threshold setting, the larger the change in the response onset time with a change in stimulus frequency. For the four ON-cell models the slopes of the OSR latency functions were measured. At a threshold of zero, the slopes ranged between 0.48 and 0.66. Making the threshold more negative increased the slope of the OSR latency function

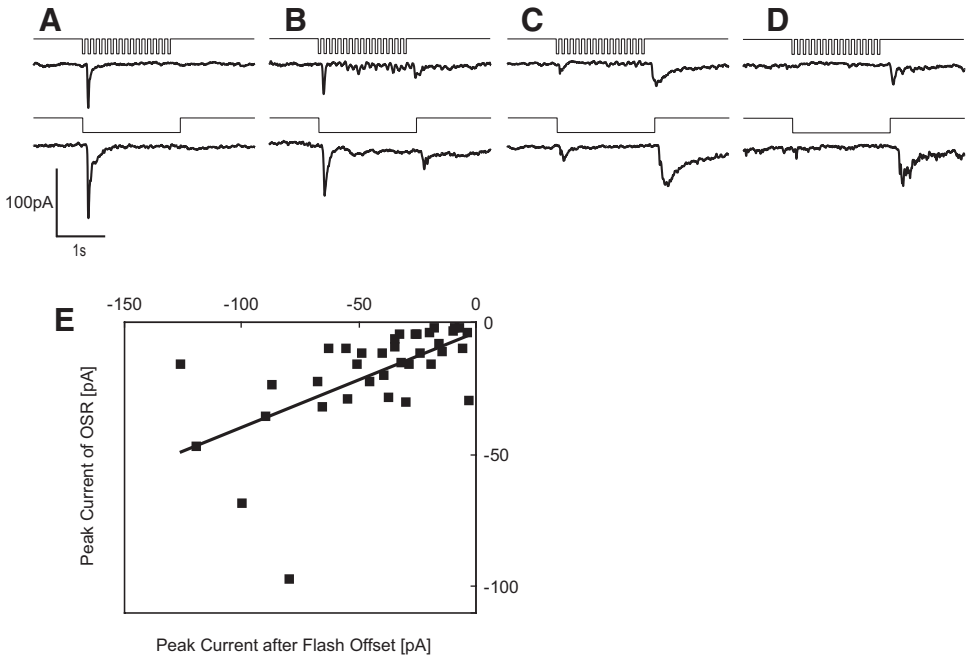

FIG. 3. Comparison of responses to a flash train (*top*) with a 2-s-long flash (*bottom*). *A*: OFF cell. *B*: OFF-dominated cell. *C*: ON-dominated cell. *D*: ON cell. *E*: the peak current of the OSR is plotted against the peak current of the offset response to a dark flash. The line describes the linear regression. The correlation between peak OSR and peak offset response is 0.6.

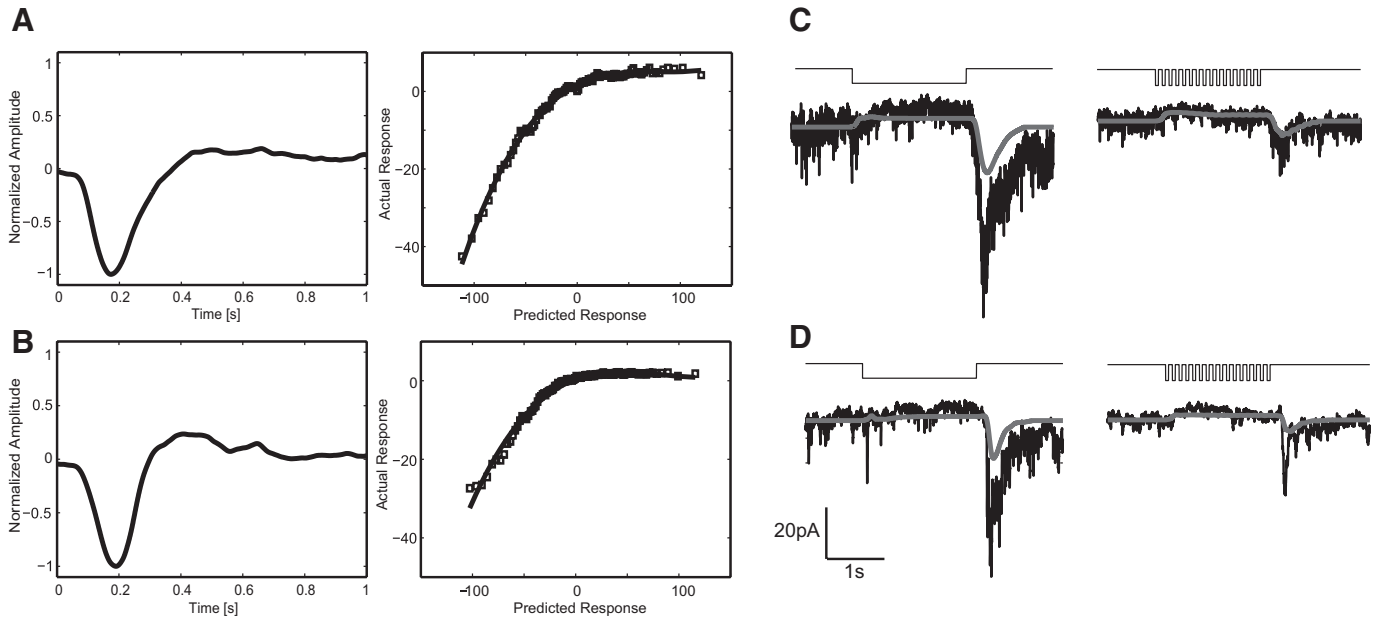

FIG. 4. The linear–nonlinear (LN) model of an ON cell predicts an OSR. *A* and *B*: LN model for 2 different ON cells calculated from stimulation with a random binary noise sequence. *C* and *D*: responses of the same cells to a dark flash (*left*) and a dark flash sequence (*right*). The current response is displayed in black; the prediction of the LN model is displayed in gray.

following the pattern shown in Fig. 5*C*. With a threshold of −3, a slope of one was produced. This change in slope happens because the steepness of the current response depends on the flash period. It takes longer for the signal to reach spike threshold for lower flash frequencies so, as the threshold is made more negative, the OSR becomes increasingly delayed with respect to its onset time for higher flash frequencies. In sum, the model simulations show that the onset of the OSR is expected to shift in time with flash frequency and that the size of the shift depends on the threshold nonlinearity that converts current to spikes.

We next explored whether the shape of the linear filter has an effect on the OSR latency function. Figure 6*A* shows the LN model of the ON ganglion cell that was used for the simulations in Fig. 5 (gray line). For these simulations a smoothed version of the ON filter was used (black line). The filter shape was

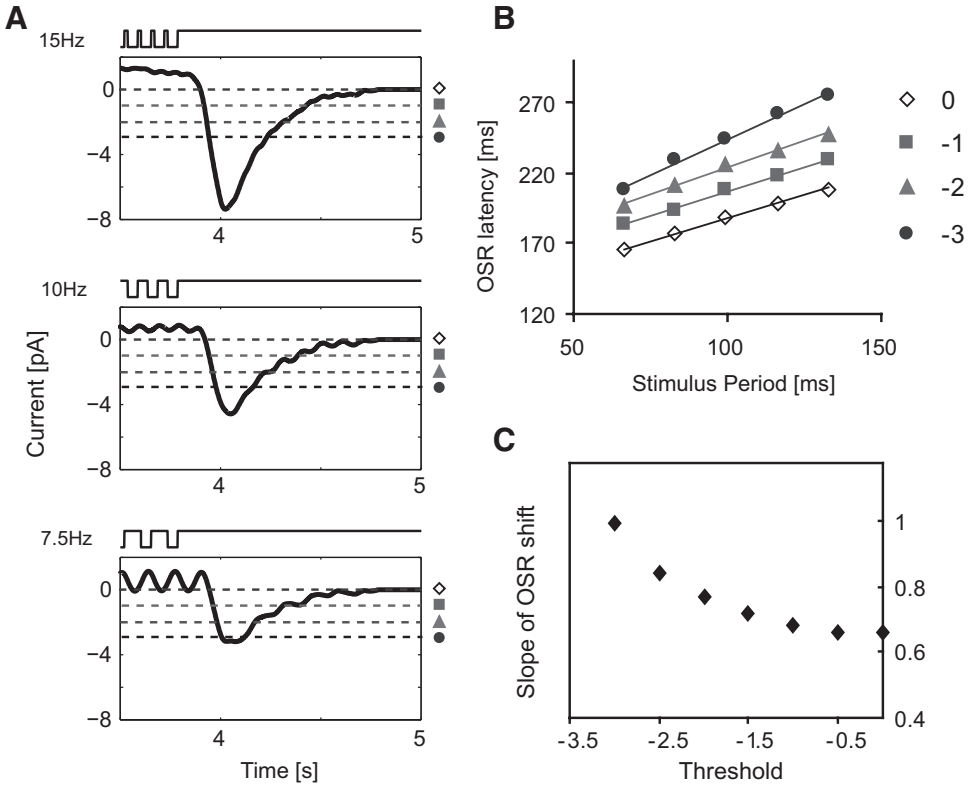

FIG. 5. The LN model predicts a temporal shift of the OSR in ON cells with a change in flash frequency. *A*: predicted responses based on the cell's LN model for flash frequencies of 15, 10, and 7.5 Hz. It can be seen that the response delay becomes larger for lower flash frequencies. The slope of the change in delay with stimulus period changes with the spike threshold. Different thresholds are indicated by dashed lines. *B*: the OSR latency is plotted against the stimulus period using different thresholds. *C*: the slope of the OSR latency function is plotted against the threshold. The more negative the threshold, the higher the slope.

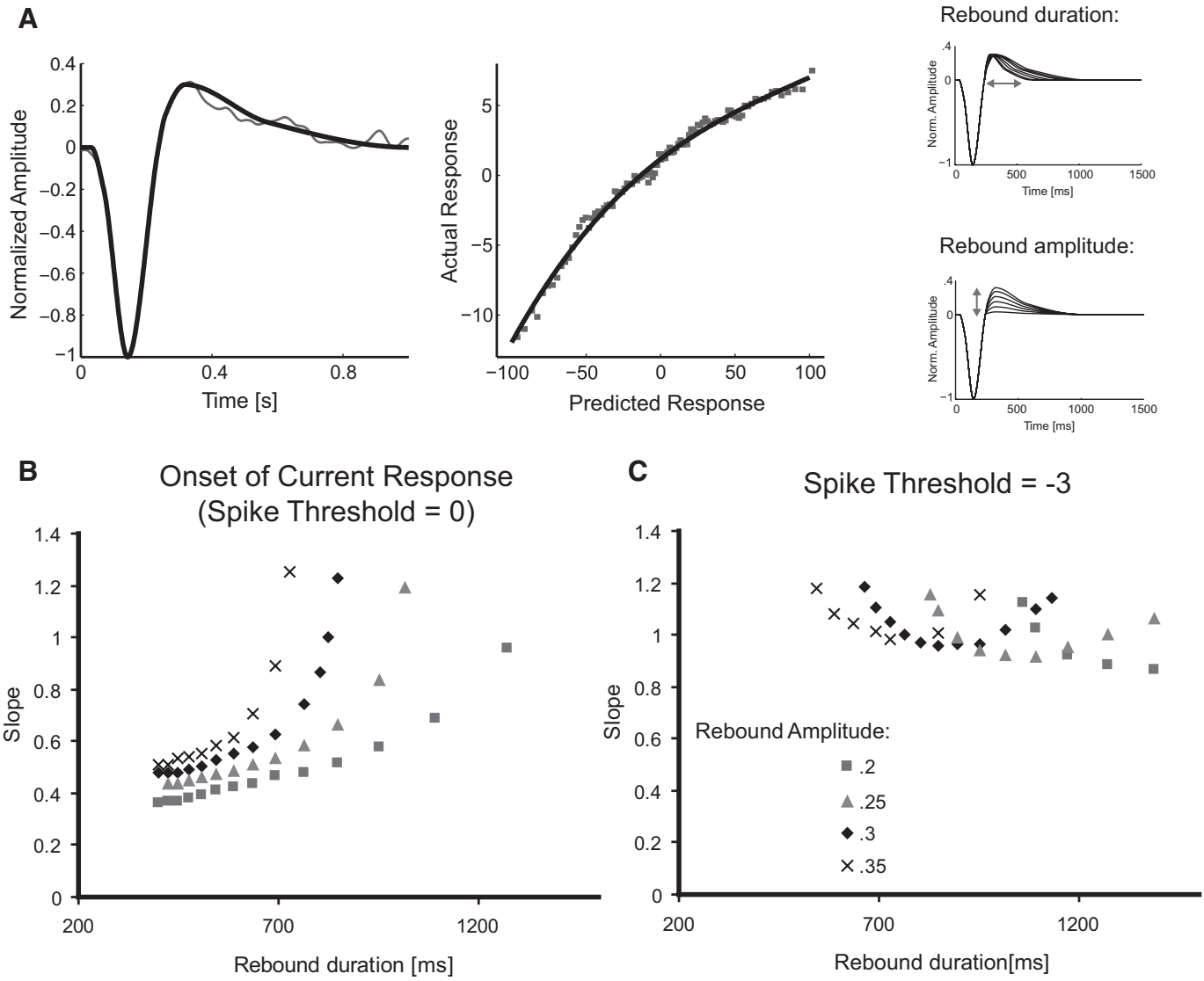

FIG. 6. The shape of the temporal filter affects the slope of the OSR latency function more strongly for current responses than for spike responses. *A*: LN model of an ON ganglion cell. In gray: normalized filter obtained from cross-correlation (*left*) and measured current plotted against the linear prediction (*right*). In black: smooth version of the LN model used for simulations. Schematic on the *far right* demonstrates how the shape of the linear filter was varied. *B*: effects of changing the filter shape on the temporal shift of the current response after a flash sequence; increasing the duration or amplitude of the rebound component of the filter leads to an increase in slope. Different symbols represent different rebound amplitudes. *C*: same as in *B* but now with a spike threshold of −3. Applying a spike threshold leads to an overall increase in slope and decreases the range of slopes one can observe.

altered by stretching or compressing the rebound component, which is responsible for causing the OSR, along the *x*-axis and the *y*-axis (as indicated to the *right* of Fig. 6*A*). To understand how filter shape alone would affect the OSR, we first performed all simulations with a spike threshold of zero. Figure 6*B* shows that varying the rebound component had a broad effect on the slope of the OSR latency function and that stretching along the *x*- or *y*-axis led to a systematic increase in the slope. We then applied a spike threshold of −3 to the current simulations, since it gave a slope of around one in Fig. 5. Figure 6*C* shows that the application of a spike threshold greatly reduced the effect of filter shape, constraining the OSR slope to values around one. The dependence on rebound duration now followed a U-shaped curve and this curve shifted downward to the right with a decrease in rebound amplitude.

A two-pathway linear–nonlinear model can reproduce ganglion cell response patterns

The OSR predicted by an LN model of an ON ganglion cell is essentially the offset response to an integrated sequence of dark flashes with a delay longer than the flash period. This model does not produce 17 responses to a 16-flash sequence nor the complex array of temporal firing patterns to such sequences that have been described for retinal ganglion cells (Schwartz and Berry 2008; Schwartz et al. 2007). Here we show that these behaviors can be explained by an ON–OFF ganglion cell model with separate LN components for the ON and the OFF pathways (Fig. 7*A*). Figure 7*B* shows the current and spike responses that the ON–OFF model predicts for a sequence of dark flashes. The OFF-pathway component is strong for the initial flashes and decays to a steady level. The ON-pathway component, which comes from the rebound phase of

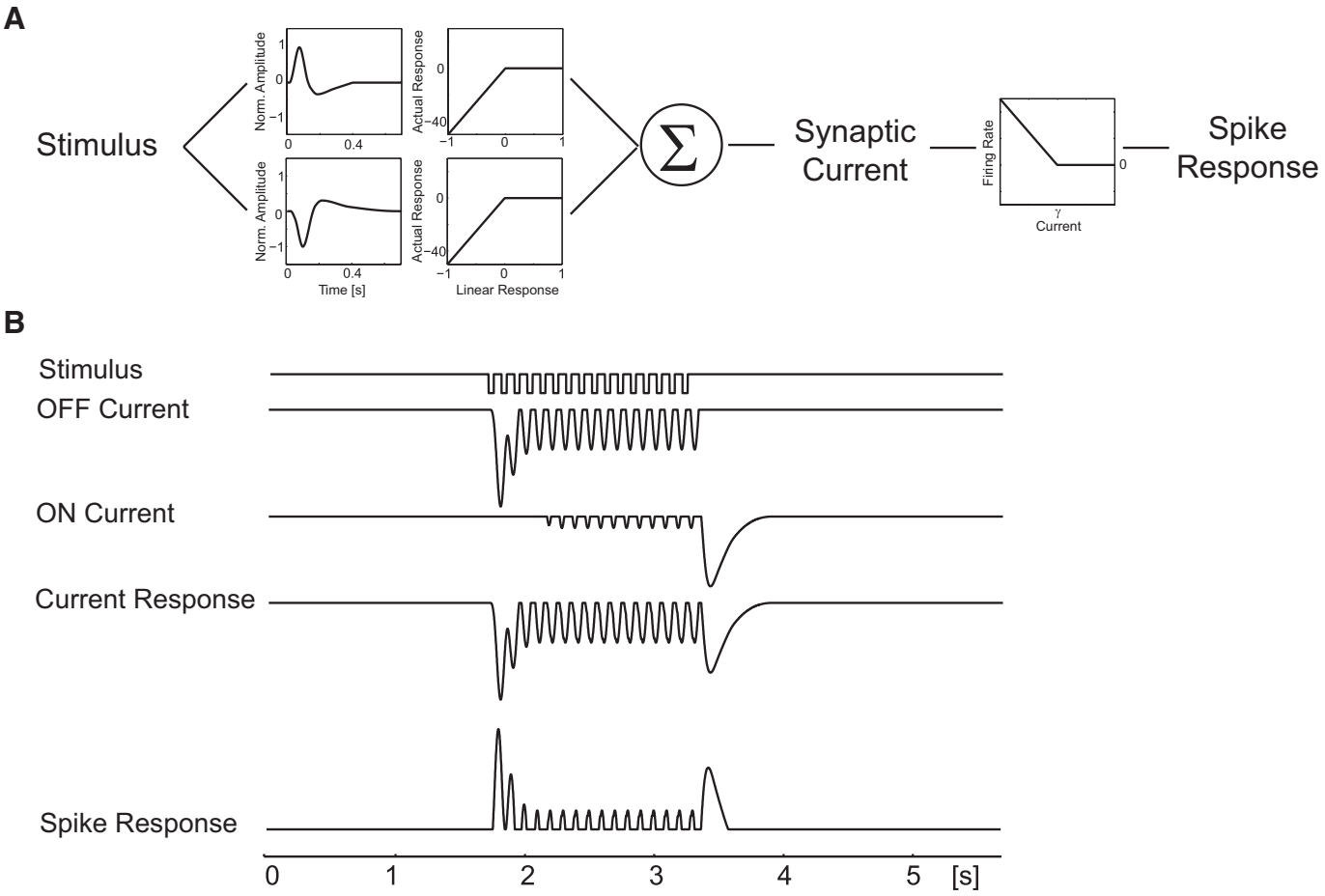

FIG. 7. ON–OFF model. *A*: the model consists of separate linear–nonlinear elements for the OFF (*top*) and the ON (*bottom*) pathways. The excitatory synaptic current is given by summing the outputs of the 2 pathways. The spiking response is modeled by applying a spike threshold. *B*: simulated response of an ON–OFF cell to a sequence of dark flashes. From *top* to *bottom*: stimulus, the response of the OFF pathway, the response of the ON pathway, the excitatory synaptic current, and the spiking response.

the ON filter, contributes little in the beginning and increases in strength over time. In the combined current response, the initial portion is therefore completely due to the OFF pathway, the OSR is due to the ON pathway, and the sustained part in the middle of the sequence is the sum of contributions from the two pathways. Application of a spike threshold then determines which response features in the combined current appear in the ganglion cell output.

By changing the gain parameters of the static nonlinearities, the relative contributions of the ON and OFF pathways can be varied and the model can produce a wide variety of complex response patterns (Fig. 8). Many of these patterns have been observed in retinal ganglion cells (Schwartz and Berry 2008). In that study, ganglion cell responses were grouped into different categories by dividing the firing profile into three epochs: the start response (to the first three flashes), the sustained response (to the remaining flashes), and the OSR (the period following the first missing flash). For each epoch five response types were identified. The start response could be "single peak," "decaying," "no response," "complex," or "facilitating." The sustained response could be "regular," "decaying," "no response," "facilitating," or "harmonic." The OSR could be "single peak," "weak response," "no response," "double peak," or "ringing." The ON–OFF model presented here can account for three of the start types: "single peak" (Fig. 8, *A*, *D*, *F*, and *G*), "decaying" (Fig. 8, *B* and *E*), and "no response" (Fig. 8*C*); for four of the sustained types: "regular" (Fig. 8*D*), "no response" (Fig. 8, *A*, *B*, *C*, and *F*), "decaying" (Fig. 8, *E* and *H*), and "facilitating" (Fig. 8*G*); and for three of the OSR types: "single peak" (Fig. 8, *B*, *C*, *D*, *F*, and *G*), "weak response" (Fig. 8*H*), and "no response" (Fig. 8, *A* and *E*). All of these response patterns can be achieved without varying the temporal dynamics of the filters, but only the parameters of the static nonlinearities (see Table 1). The "facilitating" start type can also be achieved if one allows the temporal dynamics of the OFF filter to be slower (simulations not shown). The response patterns that cannot be easily obtained with this model are a "complex" start type, "harmonic" sustained response, and "double peak" or "ringing" OSR (we return to this in the DISCUSSION). Figure 8*I* shows that one can still observe an OSR if the mean luminance of the flash sequence is kept equal to the background luminance.

Schwartz and Berry (2008) reported that none of their complex response types had any correspondence to basic response properties of ganglion cells such as the spike-triggered average and that the response to a single flash could not predict the response to a flash train. This would be expected if the cells are mostly ON–OFF cells because a linear measure like the spike-triggered average cannot predict the response of these cells. To illustrate the point we simulated

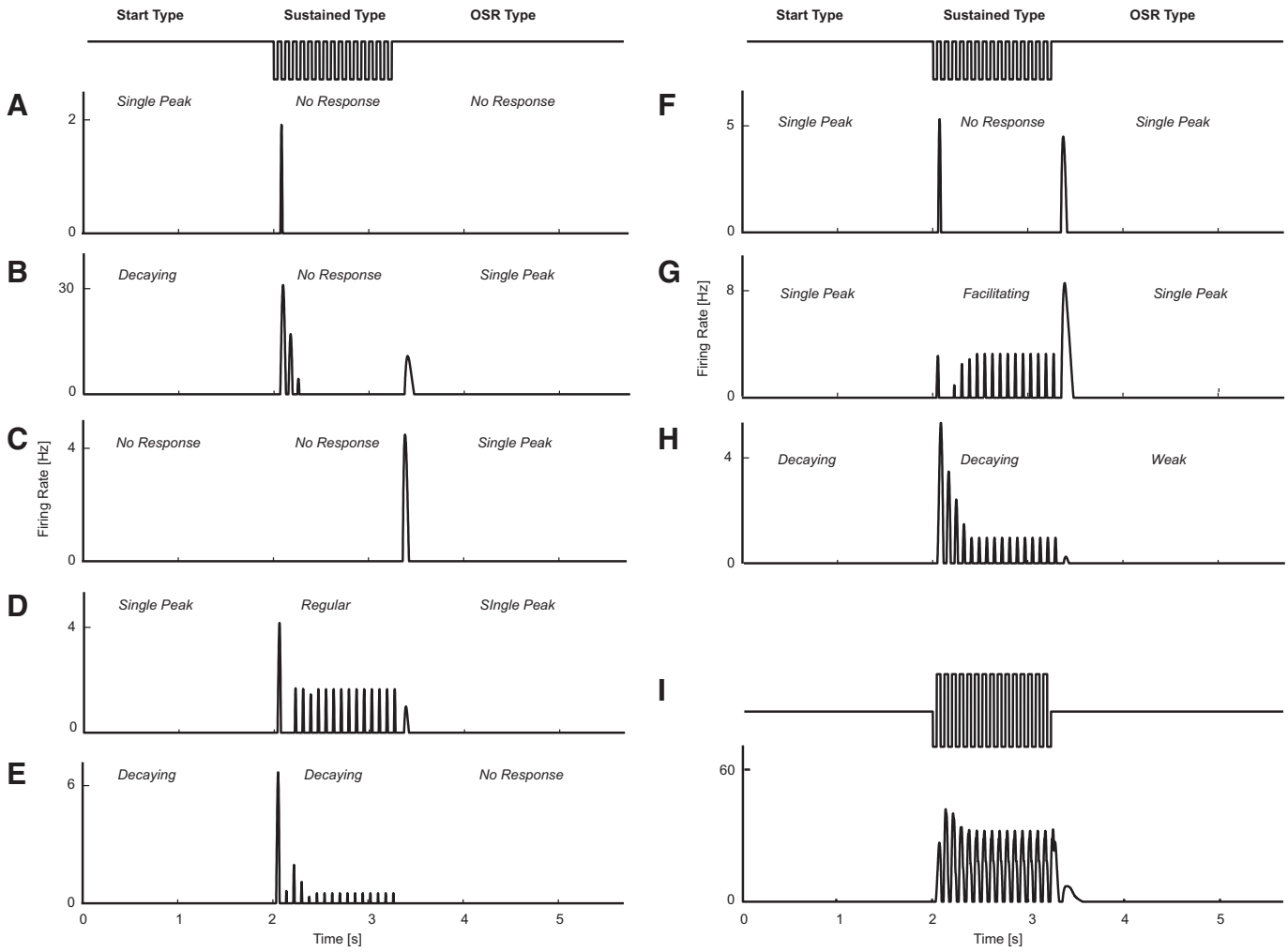

FIG. 8. ON–OFF cells can show a variety of response patterns. Flashes are shown on the *top*. *A–H*: different possible spike responses to the same flash sequence based on an ON–OFF model in which only the parameters of the static nonlinearities were varied. Different start response types: single peak (*A*, *D*, *F*, *G*), decaying (*B*, *E*, *H*), and no response (*C*); sustained response types: no response (*A*, *B*, *C*, *F*), regular (*D*), decaying (*E*, *H*), facilitating (*G*); OSR types: no response (*A*, *E*), single peak (*B*, *C*, *D*, *F*, *G*), and weak (*H*). *I*: spiking response to a stimulus in which the mean light level during the flash sequence is equal to the background luminance.

an ON–OFF cell response to a long dark flash (Fig. 9*A*), a flash sequence (Fig. 9*B*), and a fast flash (Fig. 9*C*). As Schwartz and Berry (2008) observed in their data, the model shows a double response to a brief single flash but responds only once at the beginning of the sequence and once at the end.

To confirm that most salamander ganglion cells indeed receive excitatory inputs from the ON and the OFF pathways we measured the ON–OFF indexes of a sample of 98 cells (Fig. 10). It may be seen that most cells do not have an index of +1 (ON) or −1 (OFF), nor is it often 0 (equal ON and OFF) for that matter. Thus most ganglion cells are of the ON–OFF type and the relative strength of the ON and OFF components varies between cells. This result is consistent with that obtained from sharp recordings in the eye-cup preparation and is therefore unlikely to be an artifact of recording in the slice preparation (Burkhardt et al. 1998).

TABLE 1. *Model parameters used for Fig. 8, A–I*

	Parameter				
Label	α_{ON}	β_{ON}	α_{OFF}	β_{OFF}	γ
A	0.0	0.0	0.5	0.0	−15
B	1.25	0.0	1.5	0.0	−20
C	1.0	0.0	0.0	0.0	−20
D	0.85	0.8	0.68	0.7	−3
E	1.0	1.0	1.0	1.0	−6
F	1.0	0.0	0.75	0.0	−20
G	1.5	1.5	1.0	1.0	−4
H	0.15	0.15	0.2	0.1	−1
I	2.0	0.0	1.0	0.0	−3

DISCUSSION

Our work investigated the retinal origin of the OSR, which has been described in the spike response of salamander and mouse retinal ganglion cells to a sequence of flashes (Schwartz and Berry 2008; Schwartz et al. 2007). We recorded the excitatory synaptic currents in salamander ganglion cells evoked by a dark-flash sequence and observed a current response at the end of the stimulus that fits the definition of an OSR from spike recordings. Comparing the current response to the dark-flash sequence with that to a dark flash of the same length indicates that the OSR might not be the response to an

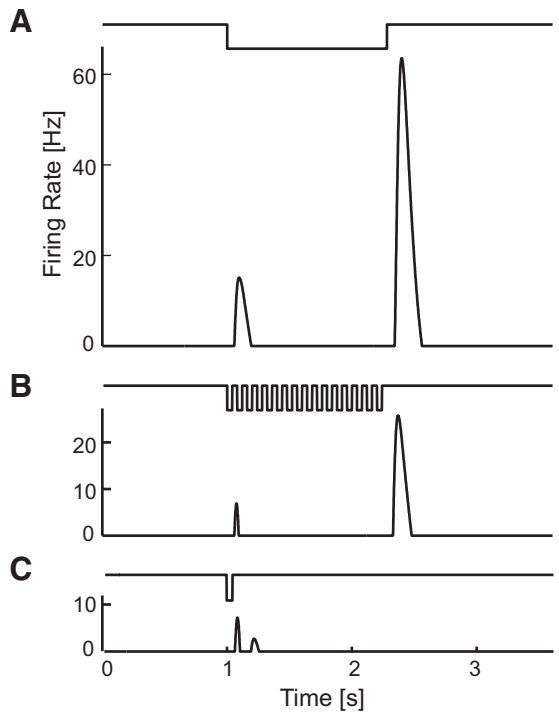

FIG. 9. Comparison of a simulated ON–OFF cell's response to a long flash (*A*), a flash train (*B*), and a single fast flash (*C*). Parameters: $\alpha_{ON} = 1.8$, $\beta_{ON} = 0$, $\alpha_{OFF} = 0.75$, $\beta_{OFF} = 0$, $\gamma = -18$.

omitted flash but is really the rebound response to the stimulus offset. Consistent with Schwartz and Berry (2008) we found that the OSR current is abolished if the ON bipolar cell pathway is blocked with L-AP4 but not if amacrine cell inhibition is blocked with γ-aminobutyric acid and glycine antagonists. The onset time of the OSR current also shifted systematically with stimulus rate and the shift persisted after blocking inhibition. However, we found that the average slope of the OSR latency function is slightly below one for the current response and varies from cell to cell. This difference is important because the functional interpretation of a slope of one is that retinal ganglion cells are predicting the omitted stimulus (Schwartz et al. 2007). It may be due to recording excitatory currents instead of extracellular spikes, given that our simulations show that a spike threshold can increase the slope and narrow the range of slopes that would be observed for cells with different temporal dynamics. It is also possible that other aspects of the spiking mechanism not implemented in our model can affect OSR timing. Whether the slope difference is truly significant is hard for us to determine because the cited studies do not report information about the variability in slope across cells.

In our simulations we showed how an LN model can predict an OSR and how the OSR can shift in time in accordance with the stimulus rate when one convolves a flash sequence with a biphasic linear filter and then applies a threshold. These results depended on several factors. First, the linear filter must have a biphasic shape to observe an OSR. Second, for dark-flash sequences, the OSR comes from the ON pathway. Third, the amplitude and duration of the rebound phase of the filter largely determine the size of the OSR time shift in the current response. Fourth, and finally, applying a threshold nonlinearity to the current response increases the slope of the OSR latency function of a given cell and decreases the variability in slope among cells with different temporal filters.

Our current recordings indicate that most ganglion cells in the salamander retina receive excitatory synaptic inputs from both the ON and the OFF pathways. Expanding our simulations to include two LN models, one for each pathway, showed how ON–OFF cells can produce an array of complicated firing profiles to a flash sequence. Many of these response patterns were described by Schwartz and Berry (2008) and could be replicated without altering the temporal dynamics of the ON or the OFF pathway. Response patterns our model could not explain have multiple peaks at the beginning of the flash sequence or during the OSR ("Complex" start type; "Ringing" and "Double Peaked" OSR types). The periodicity of the peaks was reported as evidence for an oscillatory mechanism within the ON pathway causing the OSR. However, our current recordings do not support this idea because subthreshold oscillations were not present (see Figs. 1–4). Alternative explanations for multipeaked responses at stimulus onset or offset would be that a large excitatory current elicits time-locked bursts of spikes or that a slightly delayed inhibitory current transiently interrupts spike activity (Thiel et al. 2006). Our ON–OFF model does not include direct inhibitory inputs to ganglion cells nor does it include any details of the spiking mechanism beyond a spike threshold. Incorporating them into the model would surely produce even more complex response patterns.

Implications for ON–OFF ganglion cell function

Our simulations show that the ON–OFF character of salamander ganglion cells must be taken into account to explain their multifaceted response patterns. A major challenge is how to separate the contributions of the ON and the OFF pathways. A computational separation may be possible through covariance analysis of spike (Fairhall et al. 2006; Schwartz O et al. 2006) or current responses (Werner et al. 2007), but the analysis needs large amounts of data and works only if ganglion cell input from each pathway is fully rectified,

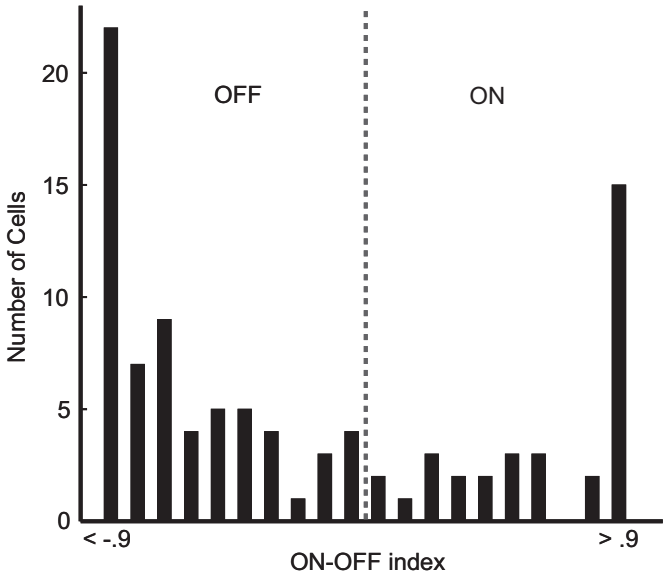

FIG. 10. Ganglion cells vary along the ON–OFF spectrum. Each bar represents the number of cells with an ON–OFF index within a certain range (bin size = 0.1).

which is unlikely to be the case for all cells; moreover, there are no good pharmacological tools to separate the two pathways. Although L-AP4 blocks the synapse between photoreceptors and ON bipolar cells, it also affects horizontal cells and photoreceptors (Hare and Owen 1992; Hirasawa et al. 2002; Takahashi and Copenhagen 1992) and the axon terminals of OFF bipolar cells (Awatramani and Slaughter 2001). Exact separation is important because the response dynamics of bipolar cells vary in each pathway, with some cells responding more transiently than others (Awatramani and Slaughter 2000; DeVries 2000), and our simulations showed how diverse ON–OFF response patterns can be obtained without even changing the dynamics of the ON or OFF filters. Moreover, ganglion cells receive direct inhibition from amacrine cells and exhibit contrast gain control (Baccus and Meister 2002; Lukasiewicz and Shields 1998; Ohzawa et al. 1985; Roska et al. 2000), which further adds to their complexity. Analyzing the circuitry of a retina that contains mainly ON–OFF ganglion cells like the salamander retina is especially challenging.

An outstanding question is why does the salamander retina contain such a diversity of ON–OFF ganglion cells? It may be that the animal is interested in motion detection of any kind and cells tuned to luminance increases or decreases are less important. Or perhaps ON–OFF cells play a part in complex computations that in more evolutionarily developed animals do not happen until visual information reaches the brain? If this were true, one might expect the computations would be carried out by distinct retinal circuits. However, our simulations demonstrate that a single ON–OFF circuit structure can account for a wide array of ganglion cell response patterns to a flash sequence, which would not be expected of cells whose behavior can be described using linear measures like the spike-triggered average. Thus although the response patterns of the retina might look complex, the underlying computational circuitry could be fairly simple. Alternatively, the diversity of ON–OFF cell responses could be related to the state of development of the eye, in that the aquatic salamander studied by us and most researchers is still in its larval stage, and it has been shown that the majority of ganglion cells in a developing retina are ON–OFF cells (Chen et al. 2008; Norman 1985; Wang et al. 2001). A recent study (Gollisch and Meister 2008) suggests that ON–OFF cells in the tiger salamander are responsible for latency coding. The authors showed that the latency of the first spike contains more information about the stimulus than the spike count and that this phenomenon is the result of different kinetics in the ON and the OFF pathways. Although further research needs to be done to understand the visual code of the tiger salamander retina, this and other recent studies (Geffen et al. 2007) make clear that including ON–OFF response characteristics is important for providing an accurate model of the majority of ganglion cells in the salamander retina.

In this study we used a 2LN model, which in its structure roughly resembles the retinal circuitry of an ON–OFF cell. The ON and OFF linear filters describe the overall kinetics of the excitatory inputs from several ON and OFF bipolar cells, respectively. The biphasic shape of the filters leads to the generation of transient responses because the sooner the filter reverses polarity, the faster the input signal decays. In the retina, transient responses are due in part to presynaptic inhibition through amacrine cells, but can also already originate at the dendritic inputs to bipolar cells (Awatramani and Slaughter 2000; Dong and Werblin 1998). The static nonlinearities in the ON and the OFF pathways summarize any nonlinear processing steps, such as contrast rectification, that happen before the signal reaches the ganglion cell. Because bipolar cell responses are thought to be fairly linear, any nonlinearities are usually attributed to mechanisms in the inner plexiform layer (Geffen et al. 2007; Gollisch and Meister 2008; Zaghloul et al. 2003).

Static nonlinearities provide an important element in shaping the response patterns of visual neurons

Nonlinearities in the signaling pathway present a problem for identifying the functional circuitry of visual neurons based on their spike responses. For example, Mechler and Ringach (2002) pointed out that complex and simple cells in the visual cortex might get their distinct spiking characteristics not from dissimilar current inputs, as often assumed, but from nonlinear transformations of current to spikes. In a similar way, our simulations exemplify how rectifying nonlinearities in the ON and the OFF pathways plus a spiking threshold can create a variety of seemingly distinct and complex response patterns in ON–OFF ganglion cells, which on a circuit level originate from a continuum of ON–OFF inputs.

At first glance, the OSR seems to support the idea of predictive coding in the retina. Here we demonstrate that this predictive coding can be obtained as a byproduct of temporal integration in a linear–nonlinear pathway. Furthermore, we show how by varying the parameters of only the static nonlinearities in a simple ON–OFF model a wide variety of seemingly complex response patterns can be obtained. This work provides insight into how a fairly simple mechanism can exhibit complicated behavior. It also illustrates how caution must be applied when attempting to infer the neural mechanisms behind a phenomenon purely from spiking responses.

ACKNOWLEDGMENTS

We thank Dr. Arash Yazdanbakhsh for helpful discussions.

GRANTS

This work was supported by a Smith Family Award and the Karl Kirchgessner Foundation.

REFERENCES

Abbott LF, Chance FS. Rethinking the taxonomy of visual neurons. *Nat Neurosci* 5: 391–392, 2002.

Awatramani GB, Slaughter MM. Origin of transient and sustained responses in ganglion cells of the retina. *J Neurosci* 20: 7087–7095, 2000.

Awatramani GB, Slaughter MM. Intensity-dependent, rapid activation of presynaptic metabotropic glutamate receptors at a central synapse. *J Neurosci* 21: 741–749, 2001.

Baccus SA, Meister M. Fast and slow contrast adaptation in retinal circuitry. *Neuron* 36: 909–919, 2002.

Belgum JH, Dvorak DR, McReynolds JS. Sustained and transient synaptic inputs to on-off ganglion cells in the mudpuppy retina. *J Physiol* 340: 599–610, 1983.

Brainard DH. The Psychophysics Toolbox. *Spat Vis* 10: 433–436, 1997.

Burkhardt DA, Fahey PK, Sikora M. Responses of ganglion cells to contrast steps in the light-adapted retina of the tiger salamander. *Vis Neurosci* 15: 219–229, 1998.

Carcieri SM, Jacobs AL, Nirenberg S. Classification of retinal ganglion cells: a statistical approach. *J Neurophysiol* 90: 1704–1713, 2003.

Chen Y, Znoiko S, Degrip WJ, Crouch RK, Ma JX. Salamander blue-sensitive cones lost during metamorphosis. *Photochem Photobiol* (March 7, 2008). doi:10.1111/j.1751-1097.2008.00310.x.

Chichilnisky EJ. A simple white noise analysis of neuronal light responses. *Network Comput Neural Syst* 12: 199–213, 2001.

Cleland BG, Levick WR. Properties of rarely encountered types of ganglion cells in the cat's retina and an overall classification. *J Physiol* 240: 457–492, 1974.

DeVries SH. Bipolar cells use kainate and AMPA receptors to filter visual information into separate channels. *Neuron* 28: 847–856, 2000.

Dong C, Werblin FS. Temporal contrast enhancement via $GABA_C$ feedback at bipolar terminals in the tiger salamander retina. *J Neurophysiol* 79: 2171–2180, 1998.

Enroth-Cugell C, Robson JG. The contrast sensitivity of retinal ganglion cells of the cat. *J Physiol* 187: 517–552, 1966.

Fairhall AL, Burlingame CA, Narasimhan R, Harris RA, Puchalla JL, Berry MJ 2nd. Selectivity for multiple stimulus features in retinal ganglion cells. *J Neurophysiol* 96: 2724–2738, 2006.

Geffen MN, de Vries SEJ, Meister M. Retinal ganglion cells can rapidly change polarity from off to on. *PLoS Biol* 5: 640–650, 2007.

Gollisch T, Meister M. Rapid neural coding in the retina with relative spike latencies. *Science* 319: 1108–1111, 2008.

Greschner M, Thiel A, Kretzberg J, Ammermuller J. Complex spike-event pattern of transient ON–OFF retinal ganglion cells. *J Neurophysiol* 96: 2845–2856, 2006.

Hare WA, Owen WG. Effects of 2-amino-4-phosphonobutyric acid on cells in the distal layers of the tiger salamander's retina. *J Physiol* 445: 741–757, 1992.

Hirasawa H, Shiells R, Yamada M. A metabotropic glutamate receptor regulates transmitter release from cone presynaptic terminals in carp retinal slices. *J Gen Physiol* 119: 55–68, 2002.

Kim KJ, Rieke F. Temporal contrast adaptation in the input and output signals of salamander retinal ganglion cells. *J Neurosci* 21: 287–299, 2001.

Lukasiewicz PD, Shields CR. Different combinations of $GABA_A$ and $GABA_C$ receptors confer distinct temporal properties to retinal synaptic responses. *J Neurophysiol* 79: 3157–3167, 1998.

Mechler F, Ringach DL. On the classification of simple and complex cells. *Vision Res* 42: 1017–1033, 2002.

Mittman S, Taylor WR, Copenhagen DR. Concomitant activation of two types of glutamate receptor mediates excitation of salamander retinal ganglion cells. *J Physiol* 428: 175–197, 1990.

Norman MF. A practical method for staging metamorphosis in the tiger salamander *Ambystoma tigrinum*. *Anat Rec* 211: 102–109, 1985.

Ohzawa I, Sclar G, Freeman RD. Contrast gain control in the cat's visual system. *J Neurophysiol* 54: 651–667, 1985.

Pang JJ, Gao F, Wu SM. Relative contributions of bipolar cell and amacrine cell inputs to light responses of ON, OFF and ON–OFF retinal ganglion cells. *Vision Res* 42: 19–27, 2002.

Rockhill RL, Daly FJ, MacNeil MA, Brown SP, Masland RH. The diversity of ganglion cells in a mammalian retina. *J Neurosci* 22: 3831–3843, 2002.

Roska B, Nemeth E, Orzo L, Werblin FS. Three levels of lateral inhibition: a space-time study of the retina of the tiger salamander. *J Neurosci* 20: 1941–1951, 2000.

Schwartz G, Harris R, Shrom D, Berry MJ 2nd. Detection and prediction of periodic patterns by the retina. *Nat Neurosci* 10: 552–554, 2007.

Schwartz GW, Berry MJ 2nd. Sophisticated temporal pattern recognition in retinal ganglion cells. *J Neurophysiol* 99: 1787–1798, 2008.

Schwartz O, Pillow JW, Rust NC, Simoncelli EP. Spike-triggered neural characterization. *J Vis* 6: 484–507, 2006.

Segev R, Puchalla J, Berry MJ 2nd. Functional organization of ganglion cells in the salamander retina. *J Neurophysiol* 95: 2277–2292, 2006.

Stone J, Fukuda Y. Properties of cat retinal ganglion cells: a comparison of W-cells with X- and Y-cells. *J Neurophysiol* 37: 722–748, 1974.

Takahashi K, Copenhagen DR. APB suppresses synaptic input to retinal horizontal cells in fish: a direct action on horizontal cells modulated by intracellular pH. *J Neurophysiol* 67: 1633–1642, 1992.

Thiel A, Greschner M, Ammermüller J. The temporal structure of transient on/off ganglion cell responses and its relation to intra-retinal processing. *J Comput Neurosci* 21: 131–151, 2006.

Troy JB, Schweitzer-Tong DE, Enroth-Cugell C. Receptive-field properties of Q retinal ganglion cells of the cat. *Vis Neurosci* 12: 285–300, 1995.

Wang GY, Liets LC, Chalupa LM. Unique functional properties of on and off pathways in the developing mammalian retina. *J Neurosci* 21: 4310–4317, 2001.

Werner B, Cook PB, Passaglia CL. Whole-cell recordings of light evoked excitatory synaptic currents in the retinal slice. *JoVE* 17, 2008. http://www.jove.com/index/Details.stp?ID=771, doi:10.3791/771.

Werner B, Cook, PB, Passaglia, CL. A continuum of on–off ganglion cells in the salamander retina. *Soc Neurosci Abstr* 391.11, 2007.

Wunk DF, Werblin FS. Synaptic inputs to the ganglion cells in the tiger salamander retina. *J Gen Physiol* 73: 265–286, 1979.

Zaghloul KA, Boahen K, Demb JB. Different circuits for ON and OFF retinal ganglion cells cause different contrast sensitivities. *J Neurosci* 23: 2645–2654, 2003.